Effect of electrostatic boundary conditions and system size on the interfacial properties of water and aqueous solutions

Cite as: J. Chem. Phys. **107**, 6342 (1997); https://doi.org/10.1063/1.474295
Submitted: 23 April 1997 • Accepted: 18 July 1997 • Published Online: 04 June 1998

E. Spohr

Effect of electrostatic boundary conditions and system size on the interfacial properties of water and aqueous solutions

E. Spohr[a)]
Department of Theoretical Chemistry, University of Ulm, Albert-Einstein-Allee 11, D-89069 Ulm, Germany

(Received 23 April 1997; accepted 18 July 1997)

The consequences of the choice of electrostatic boundary conditions on the interfacial properties of water and on the free energy of ion adsorption from aqueous solution have been investigated. The Ewald summation method for lattices, which are periodic in two dimensions, is considered to be the most adequate method in slabs of finite thickness in one dimension. In agreement with the physics of the problem a field-free region in the bulk phases is observed. The use of spherical truncation methods like the shifted-force method leads to unphysical results. The electrostatic potential depends on the size of the system. Ewald summation methods for three-dimensional lattices lead to results in qualitative agreement with the corresponding two-dimensional lattice sum. The computed value of the electrostatic potential depends on an additional parameter, namely the lattice constant c in the direction perpendicular to the interface. The results for Ewald summation in three dimensions converge to the results for Ewald summation in two dimensions for large c, the shifted-force results converge to the same limit, when the surface area of the simulation cell becomes very large and the cut-off distance increases accordingly. © *1997 American Institute of Physics.* [S0021-9606(97)51340-7]

I. INTRODUCTION

The adequate treatment of the long-range Coulomb forces is at the heart of most sophisticated computer models of polar condensed phase systems. Artificial surface effects originating from the small particle numbers in a simulation, which are mandated by finite computer resources, are usually overcome by the use of periodic boundary conditions. For periodic systems, the Ewald summation method is available to properly sum up the Coulomb interactions of the system. It is widely regarded as the most adequate treatment of the problem. Because of its computational expense many different approximations based on varying truncation or switching schemes have been proposed and used.[1,2]

Consequently, there exist a number of studies in which the effects of these truncation schemes on the simulation results have been explored. Most studies focused on systems which are periodic in all three dimensions of space (see Ref. 3–12 and references therein). Because of the isotropy of bulk liquids, spherical truncation methods often lead to qualitatively similar results as the Ewald method in three dimensions. In systems which are periodic in only two dimensions and have a finite extent in the third one the symmetry of the problem produces a nonvanishing interfacial dipole moment. In simulation studies of interfaces of electrochemical interest like liquid/liquid, liquid/solid or liquid/gas interfaces, this dipole moment is associated with the interfacial potential drop and is one of the principally interesting properties that are computed in a simulation.

In a real two-phase system the bulk phases are regions of constant electrostatic potential; they are ''field-free'' regions. In this paper it will be demonstrated that spherical truncation methods are not even approximately able to account for this fact, except at very large system sizes. It will be shown that the size of the interfacial potential drop depends on the choice of the electrostatic boundary conditions and that it is highly dependent on particle number when using spherical truncation methods. While this manuscript was prepared, Feller *et al.*[13] investigated the effects of electrostatic force truncation on, among other systems, the water/vapor and the water/lipid interface. They used a three-dimensional lattice sum. Shelley and Patey[14] investigated boundary condition effects of water confined between planar walls. They compared minimum image, spherical and cylindrical cut-off schemes with 3D Ewald summation and concluded that Ewald summation is the method of choice and that the other methods, especially the minimum image method, should be avoided. The current study goes beyond the scope of these investigations by also comparing the results obtained from two-dimensional and three-dimensional lattice summation methods. We deliberately constrain ourselves to the discussion of the interfacial polarization and focus on the interfacial electrostatic potential, because it shows most clearly that spherical truncation schemes are inadequate and that there are systematic differences between two- and three-dimensional lattice summation schemes. Many of the results are in agreement with those in reference 13 which also contains a thorough discussion of the influence of force truncation on additional structural and dynamic properties in inhomogeneous systems.

II. METHOD

A. Systems

Three different systems have been studied which have one or two liquid/solid and one or zero liquid/gas interfaces. System I is a thin film of water confined between two mer-

a)Electronic mail: eckhard.spohr@chemie.uni-ulm.de

 0021-9606/97/107(16)/6342/7/$10.00

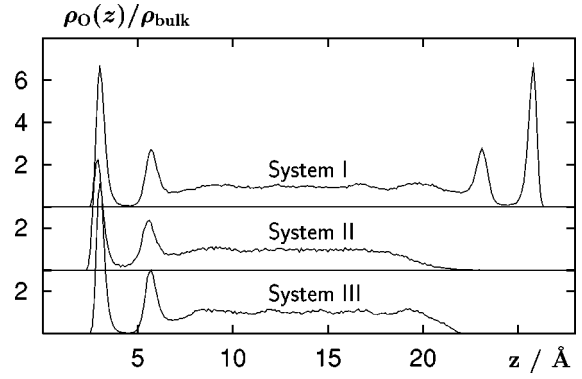

FIG. 1. Normalized oxygen density profile for the three different systems studied here. The left interface has been arbitrarily shifted to $z=0$ in all cases.

cury phases, similar to those that have been studied by Porter and Zinn in their liquid/liquid tunnel junction measurements.[15] The separation between the mercury surfaces has been adjusted during an extensive equilibration period until a bulk phase with constant liquid water density formed in the center of the film, thus correcting for the depletion of the center due to the adsorption on the mercury surface. Between 112 and 1792 water molecules were simulated. The mercury atoms have been kept at fixed positions in the form of a hcc lattice.[16]

System II is a film of 200 water molecules supported by a simple model surface. On one side of the film, adsorption of water on this ''Morse'' wall produces a liquid/solid interface; the other side forms a liquid/gas interface (see Ref. 17 for further details). System III is similar to system II. It consists of 259 water molecules and 1 fluoride ion in a film which is confined on one side by a mercury phase and on the other side by a gas phase.[18] Figure 1 illustrates the thickness of the three systems in the direction normal to the interfaces and shows the extent of density oscillations.

B. Interaction potentials

The rigid TIP4P water model[19] has been used in all studies presented here. The fluoride–water interaction potential in system III is taken from reference 20. The liquid/solid interfaces are modeled in two different ways: The model used in systems I and III is derived from *ab initio* calculations of water mercury clusters, performed on the SCF level.[21] A set of analytical pairwise additive potential functions has been fitted to the SCF data. A best fit was obtained employing the following potential functions:

$$\begin{aligned}\phi_{\text{Hg-O}}(r,\rho)=&[25518\ \exp(-2.0829r)\\&-5508.2\ \exp(-1.3922r)]f(\rho)\\&+8813.2\ \exp(-2.1759r)[1-f(\rho)],\end{aligned}\quad(1)$$

$$\phi_{\text{Hg-H}}(r)=2603.6[\exp(-2.2230r)+\exp(-2.6737r)],\quad(2)$$

$$f(\rho)=\exp(-0.2213\rho^2).\quad(3)$$

Here the energies are given in units of kJ mol^{-1} and the distances are in Å. r is the distance between two sites and $\rho=\sqrt{x^2+y^2}$ is the projection of this distance onto the plane of the interface. The total water–surface interaction energy is then obtained by summation of Eqs. (1) and (2) over all mercury atoms.

A simple external potential that incorporates the effect of surface corrugation and anisotropic adsorption was used in system II.[17] The external potential acting on the water molecules consists of a Morse function plus a corrugation term for oxygen–surface and a repulsive term for hydrogen–surface interactions:

$$V_{\text{water-surface}}=\phi_O(x_O,y_O,z_O)+\phi_H(z_{H1})+\phi_H(z_{H2}),\quad(4)$$

with

$$\begin{aligned}\phi_O(x,y,z)=&30[\exp(-2z)-2\exp(-z)]+3\exp(-2z)\\&\cdot\left[\cos\left(\frac{10\pi x}{L_x}\right)+\cos\left(\frac{10\pi y}{L_y}\right)\right]\end{aligned}\quad(5)$$

and

$$\phi_H(x,y,z)=6\ \exp(-2(z+4)).\quad(6)$$

Energies are in kJ mol^{-1} when distances are given in Å. $L_x=L_y=18$ Å are the box dimensions of the simulation cell parallel to the interfacial plane. The corrugation is felt only in the repulsive part of the Morse potential function and has a periodicity of 3.6 Å in both directions parallel to the surface, roughly corresponding to the periodicity of a Ni(100) surface. With the hydrogen–surface interactions being weakly repulsive binding occurs predominantly through the oxygen atoms. This is in keeping with experimental evidence[22] and *ab initio* calculations of transition metal water interactions.[21,23–27]

C. Electrostatic interactions

The electrostatic interactions between the point charges in the water model and the ion (in system III) have been treated in three different ways. First, to investigate the effect of smooth truncation of the interactions, the shifted-force (SF) method has been employed where the Coulomb forces are shifted by a constant amount so that they vanish at a specified cutoff radius r_c. Usually, $r_c=\frac{1}{2}\min(L_x,L_y)$. The smooth truncation is achieved by a modified potential function,

$$V_{ij}(r)=V_C(r)-V_C(r_c)-\left(\frac{\partial V_C}{\partial r}\right)_{r_c}(r-r_c),\quad(7)$$

where $V_C(r)=q_iq_j/(4\pi\epsilon_0 r)$ is the bare Coulomb potential between charges q_i and q_j at distance r with the vacuum permittivity ϵ_0. The total Coulomb energy is then

$$U=\sum_{i=1}^{N-1}\sum_{j>i}^{N}V_{ij}(r).$$

Several different algorithms have been proposed for the Ewald summation in systems periodic in two dimensions

(EW2D) with a finite extent in the third one (e.g., Refs. 28–30). According to Heyes *et al.*[28] the total Coulomb energy is given by

$$U=\frac{1}{4\pi\epsilon_0}\sum_{\mathbf{m}}^{\dagger}\sum_{i=1}^{N}\sum_{j=1}^{N} q_i q_j \frac{1}{2}\frac{\mathrm{erfc}(\alpha|\mathbf{r}_{ij}+\mathbf{m}|)}{|\mathbf{r}_{ij}+\mathbf{m}|} + \frac{1}{4\pi\epsilon_0}\sum_{i=1}^{N}\sum_{j=1}^{N} q_i q_j \sum_{\mathbf{h}>0}\frac{\pi\cos(\mathbf{h}\cdot\mathbf{r}_{ij})}{2hA} \times\left\{\exp(hz_{ij})\mathrm{erfc}\left(\alpha z_{ij}+\frac{h}{2\alpha}\right)+\exp(-hz_{ij}) \times\mathrm{erfc}\left(-\alpha z_{ij}+\frac{h}{2\alpha}\right)\right\} - \frac{1}{4\pi\epsilon_0}\sum_{i=1}^{N}\sum_{j=1}^{N} q_i q_j \frac{\pi}{A} \times\left[z_{ij}\mathrm{erf}(\alpha z_{ij})+\frac{1}{\alpha\sqrt{\pi}}\exp[-(\alpha z_{ij})^2]\right] - \frac{1}{4\pi\epsilon_0}\frac{\alpha}{\sqrt{\pi}}\sum_{i=1}^{N} q_i^2 . \tag{8}$$

In three dimensions, the Ewald technique[1] yields the corresponding formula (EW3D)

$$U=\frac{1}{4\pi\epsilon_0}\sum_{\mathbf{n}}^{\dagger}\sum_{i=1}^{N}\sum_{j=1}^{N} q_i q_j \frac{1}{2}\frac{\mathrm{erfc}(\alpha|\mathbf{r}_{ij}+\mathbf{n}|)}{|\mathbf{r}_{ij}+\mathbf{n}|} + \frac{1}{\epsilon_0 V}\sum_{\mathbf{k}>0}\frac{1}{k^2}e^{-\frac{k^2}{4\alpha^2}}\left\{\left|\sum_{i=1}^{N} q_i\cos(\mathbf{k}\cdot\mathbf{r}_i)\right|^2 + \left|\sum_{i=1}^{N} q_i\sin(\mathbf{k}\cdot\mathbf{r}_i)\right|^2\right\} - \frac{1}{4\pi\epsilon_0}\frac{\alpha}{\sqrt{\pi}}\sum_{i=1}^{N} q_i^2 . \tag{9}$$

Here $\mathbf{r}_{ij}$ is the distance vector between charges q_i and q_j at Cartesian coordinates $\mathbf{r_i}$ and $\mathbf{r_j}$, and z_{ij} is its normal component. $\mathbf{m}$ and $\mathbf{n}$ are real-space lattice vectors for the two-dimensional and three-dimensional system, respectively, and $\mathbf{h}$ and $\mathbf{k}$ are reciprocal lattice vectors for the two-dimensional and three-dimensional system, respectively, with the corresponding moduli m, n, h, and k. N is the total number of charges, A and V the area and the volume of the two-dimensional and three-dimensional unit cells, respectively. The ''daggered'' summation indicates omission of the $i=j$ term when $\mathbf{n}=0$ or $\mathbf{m}=0$. α is the separation parameter that controls the convergence of real space and reciprocal space sums. It is usually chosen in such a way that the real-space sum is converged when using the minimum image convention. Intramolecular site–site Coulomb interactions, which are not part of the model, are implicitly included in the above formula and need to be subtracted separately.

The two-dimensional Ewald method in the form of Eq. (8) is computationally expensive because of the double sum in reciprocal space. The computationally more efficient method due to Hautman and Klein[30] is only applicable for ''flat'' systems where the extent of the z dimension is small compared to that in the x and y direction. Without modification, the two-dimensional Ewald sum, which has not been optimized, is more than 10 times more expensive for the systems studied here than an optimized three-dimensional Ewald scheme. Therefore, the two-dimensional Ewald calculations were performed by interpolation from a table of potential energy, forces and second derivatives on a three-dimensional grid with spacing of about 0.2 Å. For small distances ($r<3.3$ Å), the interactions were calculated directly from Eq. (8). For $\Delta z>\min(L_x,L_y)$ the ''parallel plate capacitor'' approximation ($F_z\approx q_i q_j/(2\epsilon_0 L_x L_y)$; $F_x=F_y\approx 0$) has been applied. The approximations lead to a relative mean square deviation between calculated and exact total forces of less than about 0.001. In one case (system III, 112 molecules) we have compared the approximations with a simulation using Eq. (8) directly and found no differences in the calculated properties. The three-dimensional Ewald calculations were made using Eq. (9) without modifications.

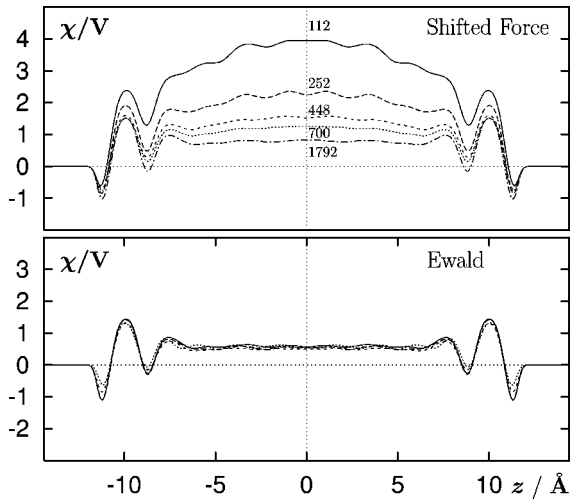

FIG. 2. Plot of the electrostatic potential $\chi(z)$ across laminae of liquid water of 28.8 Å thickness between two model mercury surfaces (system I). Simulations lasted between 40 (for the large systems) and 300 picoseconds (for the smallest) after equilibration. Top: The shifted-force (SF) method has been used together with the minimum image convention; the number of particles, which is directly proportional to the surface area of mercury in the basic simulation cell, is indicated. The cut-off radius is 5.2, 7.8, 10.4, 13.0, and 20.8 Å for particle numbers of 112, 252, 448, 700, and 1792, respectively. Bottom: the two-dimensional Ewald summation (EW2D) has been used; the four different curves correspond to simulations of 112, 252, 448, and 700 water molecules.

The equations of motion of the rigid molecules and atoms have been integrated by the SHAKE constraint algorithm and the VERLET algorithm, respectively,[1] using a time step length of 2.5 fs. The kinetic temperature was kept constant at 298.15 K by coupling to a Berendsen thermostat[31] with a time constant of 0.4 ps.

III. RESULTS

A. Comparison between shifted-force method and Ewald summation in 2 dimensions

In the following, differences in simulations of slabs of pure water confined between two mercury phases are calculated when using the shifted-force (SF) method[32] and the

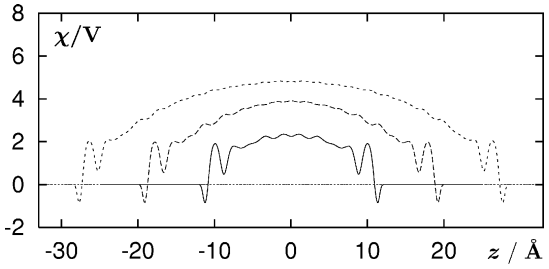

FIG. 3. Plot of the electrostatic potential $\chi(z)$ across water laminae of varying width between two model mercury surfaces, using the SF method. The cross section is $L_x \times L_y = 18 \times 15.59 \text{Å}^2$ in all cases. The full line is from the simulation with 252 particles, which is also depicted in Fig. 2. The two dashed lines are from simulations of 400 and 560 water molecules, using the same values of L_x und L_y. Simulations lasted for 80, 60, and 40 ps for the 252, 400, and 560 water systems, respectively, after equilibration.

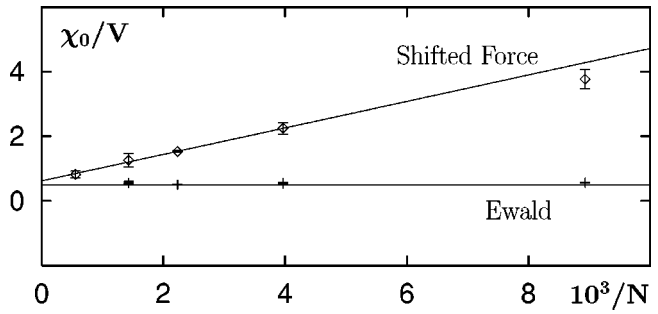

FIG. 4. A plot of the electrostatic potential χ_0 in the center of a lamina of water between two mercury phases, which are 28.8 Å apart, as a function of the reciprocal number of particles. The number of particles is proportional to the surface area of the crystal lattices in the basic simulation box. Crosses and diamonds represent EW2D and SF simulations, respectively.

two-dimensional Ewald summation (EW2D) according to Eq. (8). Figure 2 shows the electrostatic potential,

$$\chi(z) = -\frac{1}{\epsilon_0}\int_0^z \rho_c(z')(z-z')dz' \tag{10}$$

as a function of coordinate z where $\rho_c(z')$ is the charge density at location z' produced by the partial charges of the water model. The distance between the mercury phases is 28.8 Å. The top frame shows the SF results, where the cutoff radius is half the minimum box-size in the lateral directions. The bottom frame shows the EW2D results. No image forces between charges in the liquid phase and their images in the metal are taken into account in this study.

The dimension of the basic simulation cell in the lateral dimension has been varied systematically. At typical system sizes with slabs consisting of several hundred water molecules, there is obviously a large size dependence in the SF data (see below). The value of χ_0 in the center of the lamina is significantly larger than in the case of the Ewald summation where no size dependence exists within the limits of statistical uncertainties. Even at very small box sizes in the lateral directions (for 112 water molecules, $L_x/2 = 5.2$ Å; oscillations in water–water pair correlation functions persist to much larger distances) the electrostatics of the ''bulk''-like central part of the lamina is described correctly. On the other hand, even for the largest SF system (1792 water molecules; much less molecules are employed in typical simulations) the value of χ_0 still differs from the value of the smallest EW2D system by about 0.25 V.

Furthermore, in the ''bulk'' region, -5 Å$<z<5$ Å, the mean electrostatic potential is not constant for the SF simulations: an artificial mean electric field exists at each location in the lamina, which is, however, rather small for the biggest simulation cell. Figure 3 shows that the electric field in the SF simulations persists even when the distance between the two interfaces is increased significantly at a constant lateral dimension. Consequently, the potential drop in the center of the lamina depends not only on the surface area but also on the distance between the two interfaces.

System size effects in aqueous systems have generally been studied much less systematically than in the case of unpolar model liquids in two and three dimensions or in the case of phase transitions.[33] Figure 4 plots the electrostatic potential, χ_0, in the center of the water slabs versus reciprocal particle number (which is proportional to the reciprocal surface area, since the thickness of the slab is the same in all cases). Like in bulk systems,[3] the size dependence is small in the EW2D simulations. When long-range forces are neglected, the polarization of the slab becomes strongly size dependent in the SF series. Extrapolation to infinite slab cross section ($\lim 1/N \to 0$) leads to results in agreement with the Ewald summation. However, the asymptotic value of the electrostatic potential is reached only for systems with about 10^4 molecules, while as few as 10^2 molecules are sufficient to adequately describe the electrostatic properties of the interface by using Ewald summation.

B. Two-dimensional versus three-dimensional Ewald summation

Several authors have used the Ewald summation method for systems which are periodic in three dimensions to simulate liquid films which are periodic only in two dimensions. In these cases the box-size in the z-direction is artificially defined as being a factor of, say, 3 larger than in the other directions. In Ref. 13 a field-free bulk-like region has been observed with this setting. Figure 5 demonstrates that indeed a field-free region can be obtained in this way, but that the size of the computed potential drop across any interface depends on the size of the periodic box in the z-direction. The figure shows the results for a film of 200 water molecules on a Morse surface (system II) from Ewald summation in two dimensions (full line with diamonds; EW2D) together with those from three-dimensional Ewald summations, where the periodic box is elongated in the z-direction by a factor of 3 (full line; EW3DX3) or 5 (dashed line; EW3DX5) relative to the dimension in the x- and y-directions (18 Å).

Elongation of the box by a factor of 3 leads to a substantially lower value of the electrostatic potential in the liquid phase; in addition, the overall potential drop across the entire film is significantly different from the value in the 2-dimensionally periodic system. When increasing the lattice constant in the z-direction even further (to 90 Å or 5 times

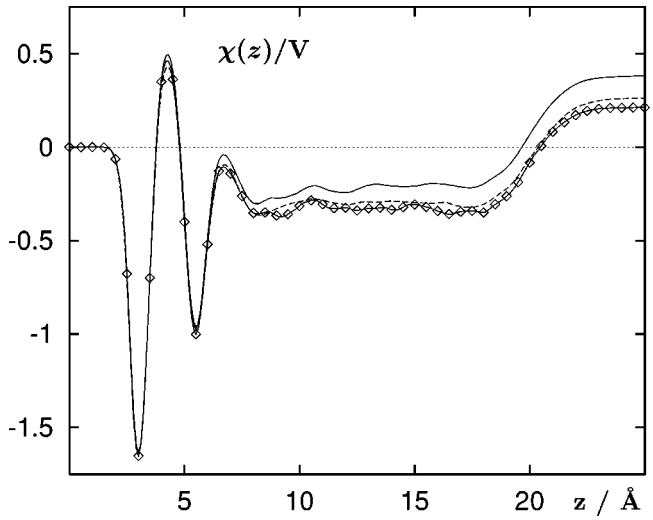

FIG. 5. Electrostatic potential functions $\chi(z)$ in system II. The Coulomb interactions have been calculated by Ewald lattice summation methods for a truly 2-dimensional periodic lattice (EW2D, full line with diamonds) and for three-dimensional lattices with lattice constants $L_z=3\times L_x$ (EW3DX3, full line) and $L_z=5\times L_x$ (EW3DX5, dashed line). All simulations lasted for 200 ps after equilibration.

the lateral box dimension) the potential function obtained by the three-dimensional lattice sum is almost identical to the one for system EW2D. The potential curves converge, as might be expected, with an increasing lattice constant (see the discussion below).

C. Free energy of ion adsorption

The free energy of adsorption of single ions near a model electrode surface has been calculated by several groups using umbrella sampling or constrained molecular dynamics methods. Truncation schemes[18,34–40] and Ewald summation[17] have been used. It is generally assumed that the adsorption of simple ions on metal surfaces is governed by electrostatic (energy of hydration) and steric phenomena (work of hole formation). In Ref. 37 it was proposed that the pure solvent contribution to the free energy of ion adsorption could be combined *a posteriori* (i.e., after the simulation) with the direct contribution (from ion–metal interactions) to obtain the total free energy. The solvent contribution was combined with the direct interactions from quantum chemical calculations and from the simple image model. While this approach may be useful in connection with the quantum mechanical model, the procedure neglects screening when using the image model.

In a subsequent calculation,[41] the image interactions have been switched on already during the simulation, so that solvent screening can take place. Figure 6 compares, for the case of the fluoride ion, the pure solvent contribution to the free energy, obtained in a SF simulation without image charges (dashed line), with the total free energy of adsorption, obtained in an EW2D simulation with image charges (full line). Both curves are very similar, except for the region of contact adsorption. The similarity is the consequence of the screening of the image charge by the solvent molecules.

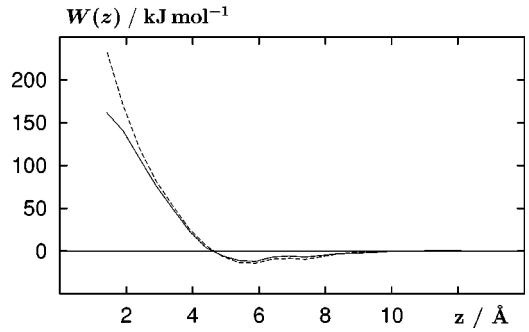

FIG. 6. Free energy of adsorption of a fluoride ion near a mercury surface. Full line: EW2D simulation with image charges; dashed line: SF simulation without image charges; the image plane is located at $z=0$. Both simulations lasted for 70 ps after equilibration.

If at least one layer of solvent molecules is between the ion and the metal surface, the high dielectric constant of water will substantially reduce the electric field originating from the surface charge (as represented by the assembly of image charges). Although the screening cannot be complete, the accuracy of the free energy calculations is apparently not sufficient to distinguish clearly between the two systems. Only at small differences, where the solvent screening becomes ineffective, the two systems are different; the self-image attraction acting on the ion becomes dominant and leads to a less repulsive free energy curve (full line).

Figure 7 shows the solvent contribution to the electrostatic potential in two different simulations, when the ion is held fixed at $z=7$ Å. It becomes clear that similar free energy curves are the result of very different electric fields and potentials in the liquid phase. The EW2D simulation does produce a bulk field-free region in the range between 10 and 20 Å, whereas the SF simulation does not. Direct simulations by Glosli and Philpott give no indication either that there are significant differences between the adsorption behavior of Li^+ and I^- when potential truncation[42] or Ewald summation[43] is used for the Coulomb interactions. The details of the electrostatics are obviously not very important here.

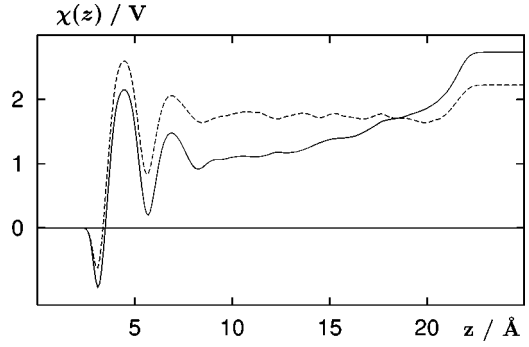

FIG. 7. The solvent contribution to the electrostatic potential of system III with one fluoride ion at $z=7$ Å. Full line: SF, dashed line: EW2D.

IV. SUMMARY AND DISCUSSION

A comparative study of the effect of the treatment of the long-range Coulomb forces in simulations of electrochemical interfaces was performed. The Ewald summation method for systems periodic in two directions of space and of finite extent in the third direction (EW2D) is taken as reference, because it exhibits the asymptotically correct boundary conditions of a liquid slab confined by 2 planar interfaces. The center of the slab must be a field-free region with constant electrostatic potential, provided the slab is thick enough. We focused on the examination of the electrostatic properties of the liquid phase, since it is the most sensitive probe for the impact of the different schemes.

Spherical truncation methods, like the SF procedure, lead to physically incorrect behavior for most of the commonly studied systems. The region of constant density in a film of water is not field-free (Figs. 2 and 3). Furthermore, a very strong system size effect is evident. In this case, the magnitude of the interfacial potential depends on the interface area of the basic simulation cell (which defines the cut-off radius) as well as on the separation between interfaces. It was demonstrated that the SF results approach the correct limiting value of the EW2D method for large cut-off radii (i.e., large interface areas). From Fig. 4 one can estimate that shifted-force calculations in a box of dimension 60×60 Å^2 should approximate the Ewald summation result. While such a system can in principle be simulated, it is presently not a routine calculation and it would be more expensive to carry out than one of the small Ewald calculations which are already converged with respect to system size. The reason for the shortcomings of the SF method is that, contrary to homogeneous and isotropic bulk systems, a significant net polarization occurs at every interface. The electrostatic interaction of any species in the slab with such a polarized interface is necessarily strongly dependent on truncation or the consideration of long-range interactions. Spherical truncation methods lead to a systematic bias, not only in the computed energies but also in the forces that govern the molecular dynamics, because a certain number of (either predominantly repulsive or predominantly attractive) interactions are neglected.

Figure 8 illustrates the differences in the pair forces between the various methods employed in the present study. It shows the relative change in force if two charges are separated in a direction perpendicular to the interfacial plane. The correct long-range limit for a system periodic in two directions is that the force approaches the constant value $F_z = q_i q_j/(2\epsilon_0 L_x L_y)$. This is a consequence of the fact that, if the distance z is large compared to the lattice dimensions (L_x, L_y) parallel to the interface, the point-charge nature of the two charges becomes irrelevant and the two charges interact like the two charged surfaces of a parallel plate capacitor (which forms the basis of the approximation in section II C). The SF method and the bare Coulomb force deviate strongly from the correct value, which is the microscopic reason for the incorrect behavior of systems subjected to spherical truncation methods.

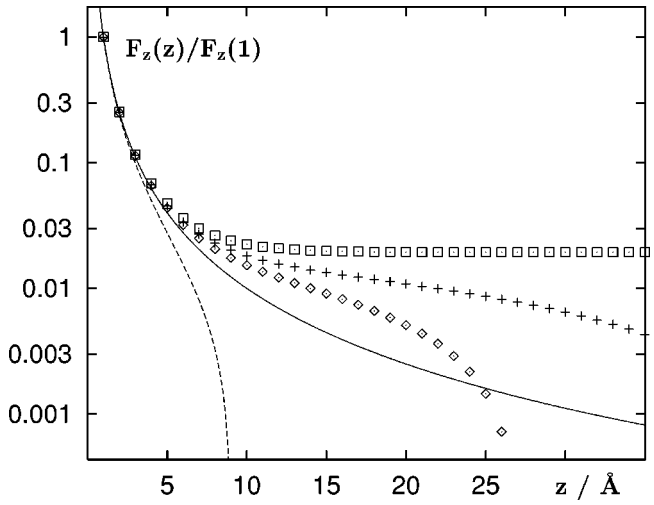

FIG. 8. Coulomb forces (logarithmic scale) between two unit point charges at (0,0,0) and (0,0,z) obtained from various treatments of the Coulomb interactions in a simulation cell with $L_x = L_y = 18$ Å. Full line: bare Coulomb force; dashed line: shifted-force (SF) with cut-off $r_c = 9$ Å; diamonds and crosses: 3-dimensional Ewald sum with $L_z = 3\times L_x$ (EW3DX3) and with $L_z = 5\times L_x$ (EW3DX5), respectively; squares: 2-dimensional Ewald sum (EW2D).

Figure 8 also shows that there are discrepancies between the microscopic forces obtained by the two Ewald summation methods. The deviations of the EW3DXn methods from the EW2D methods originate from the coupling between the periodic replicas of the interface. With increasing lattice parameter L_z the EW3D pair force traces the EW2D force more closely. Since the long-range lateral interactions within the interface are correctly accounted for in the EW3DXn ($n=3$, 5) simulations, a field-free region is also observed in the EW3D simulations. The unphysical coupling between replicas of the interfacial dipole is responsible for the small quantitative differences between the computed potential drops. This coupling decreases with increasing parameter L_z (compare Fig. 5). At the same time, however, the three-dimensional Ewald summation method becomes computationally inefficient due to the large number of reciprocal space vectors needed for convergence in Eq. (9). The tabulated two-dimensional Ewald summation (EW2D) needs about the same computer time for system I than the Ewald summation EW3DX3. EW3DX5 is about 15% more expensive, while SF calculations are about an order of magnitude faster. It should be noted that Berkowitz and coworkers do also find a field-free region,[44] using the method of dipolar sheets by Aloisi *et al.*[45] to correct for the long-range interactions.

From the discussion and further data not presented here it can be concluded that pair correlation functions, atom density profiles, charge densities, dipole densities, and dipole distributions are not very sensitive to the choice of boundary condition. This is equivalent to stating that the small differences are usually not resolved due to statistical error. Free energy and force profiles also appear to be not very sensitive, at least at larger distances. On the other hand, integrated quantities, especially the electrostatic potential, magnify the

differences between the different methods. The available data on self diffusion coefficients and dipolar relaxation times are inconclusive and do not exhibit a systematic dependency on boundary conditions.

In summary, the calculations show that the choice of the boundary conditions for Coulomb forces is crucial to achieve a physically correct microscopic model of the electrochemical interface, especially when electrostatic information is to be obtained. The Ewald summation for systems with two-dimensional periodicity and finite thickness in the third dimension is demonstrated to be the adequate method; simulations on the basis of truncation or three-dimensional Ewald methods are shown to converge slowly to the EW2D results with increasing system size. On the other hand, many properties like, e.g., hydration shell structures, atom density profiles, preferential loci of ion adsorption, or pair correlation functions, do not depend as strongly on the treatment of long-range interactions and can be calculated with less computationally demanding techniques.

ACKNOWLEDGMENTS

Financial support by the Fonds der Chemischen Industrie and helpful discussions with M. R. Philpott, M. L. Berkowitz, and A. Kohlmeyer are gratefully acknowledged.

[1] M. P. Allen and D. J. Tildesley, *Computer Simulations of Liquids* (Oxford University Press, New York, 1987).
[2] R. Haberlandt, S. Fritzsche, G. Peinel, and K. Heinzinger, *Molekulardynamik. Grundlagen und Anwendungen* (Vieweg Braunschweig, Wiesbaden, 1995).
[3] C. G. Gray, Y. S. Sainger, C. G. Joslin, P. T. Cummings, and S. Goldman, J. Chem. Phys. **85**, 1502 (1986).
[4] P. Linse and H. C. Andersen, J. Chem. Phys. **85**, 3027 (1986).
[5] J. A. Barker, Mol. Phys. **83**, 1057 (1994).
[6] L. Perera, U. Essmann, and M. L. Berkowitz, J. Chem. Phys. **102**, 450 (1995).
[7] J. E. Roberts and J. Schnitker, J. Phys. Chem. **99**, 1322 (1995).
[8] K. Esselink, Comput. Phys. Commun. **87**, 375 (1995).
[9] J. D. Madura and B. M. Pettitt, Chem. Phys. Lett. **150**, 105 (1988).
[10] C. L. Brooks III, B. M. Pettitt, and M. Karplus, J. Chem. Phys. **83**, 5897 (1985).
[11] K. Tasaki, S. Mcdonald, and J. W. Brady, J. Comput. Chem. **14**, 278 (1993).
[12] T. A. Andrea, W. C. Swope, and H. C. Andersen, J. Chem. Phys. **79**, 4576 (1983).
[13] S. E. Feller, R. W. Pastor, A. Rojnuckarin, S. Bogusz, and B. R. Brooks, J. Phys. Chem. **100**, 17 011 (1996).
[14] J. C. Shelley and G. N. Patey, Mol. Phys. **88**, 385 (1996).
[15] J. D. Porter and A. S. Zinn, J. Phys. Chem. **97**, 1190 (1993).
[16] J. Böcker, R. R. Nazmutdinov, E. Spohr, and K. Heinzinger, Surf. Sci. **335**, 372 (1995).
[17] E. Spohr, J. Mol. Liquids **64**, 91 (1995).
[18] E. Spohr, Acta Chem. Scand. **49**, 189 (1995).
[19] W. L. Jorgensen, J. Chandrasekhar, J. D. Madura, R. W. Impey, and M. L. Klein, J. Chem. Phys. **79**, 926 (1983).
[20] S. H. Lee and J. C. Rasaiah, J. Chem. Phys. **101**, 6964 (1994).
[21] R. R. Nazmutdinov, M. Probst, and K. Heinzinger, J. Electroanal. Chem. **369**, 227 (1994).
[22] P. A. Thiel and T. E. Madey, Surf. Sci. Rep. **7**, 211 (1987).
[23] S. Holloway and K. H. Bennemann, Surf. Sci. **101**, 327 (1980).
[24] H. Yang and J. L. Whitten, Surf. Sci. **223**, 131 (1989).
[25] M. W. Ribarsky, W. D. Luedtke, and U. Landman, Phys. Rev. B **32**, 1430 (1985).
[26] H. Sellers and P. V. Sudhakar, J. Chem. Phys. **97**, 6644 (1992).
[27] M. Rosi and C. W. Bauschlicher, Jr., J. Chem. Phys. **90**, 7264 (1989).
[28] D. M. Heyes, M. Barber, and J. H. R. Clarke, J. Chem. Soc. Faraday Trans. II **73**, 1485 (1977).
[29] Y.-J. Rhee, J. W. Halley, J. Hautmann, and A. Rahman, Phys. Rev. B **40**, 36 (1989).
[30] J. Hautman and M. L. Klein, Mol. Phys. **75**, 379 (1992).
[31] H. J. C. Berendsen, J. P. M. Postman, W. F. van Gunsteren, A. DiNola, and J. R. Maak, J. Chem. Phys. **81**, 3684 (1984).
[32] W. B. Streett, D. J. Tildesley, and G. Saville, Mol. Phys. **35**, 639 (1978).
[33] *The Monte Carlo Method in Condensed Matter Physics*, Vol. 71 of Topics in Applied Physics, edited by K. Binder (Springer-Verlag, Berlin, 1992).
[34] I. Benjamin, J. Chem. Phys. **95**, 3698 (1991).
[35] M. A. Wilson and A. Pohorille, J. Chem. Phys. **95**, 6005 (1991).
[36] D. A. Rose and I. Benjamin, J. Chem. Phys. **95**, 6956 (1991).
[37] E. Spohr, Chem. Phys. Lett. **207**, 214 (1993).
[38] L. Perera and M. L. Berkowitz, J. Phys. Chem. **97**, 13 803 (1993).
[39] D. A. Rose and I. Benjamin, J. Chem. Phys. **98**, 2283 (1993).
[40] D. A. Rose and I. Benjamin, J. Chem. Phys. **100**, 3545 (1994).
[41] E. Spohr (unpublished).
[42] J. N. Glosli and M. R. Philpott, J. Chem. Phys. **98**, 9995 (1993).
[43] J. N. Glosli and M. R. Philpott, in *Microscopic Models of Electrode–Electrolyte Interfaces*, edited by J. W. Halley and L. Blum (Electrochemical Society Inc., Pennington, 1993), No. 93-5, pp. 90–103.
[44] M. L. Berkowitz (personal communication).
[45] G. Aloisi, M. L. Foresti, R. Guidelli, and P. Barnes, J. Chem. Phys. **91**, 5592 (1989).